The Research on Optimal Tropospheric Combined Model Based on Multi-GNSS PPP

Guoqiang Jiao[1,2], Shuli Song[1(✉)], Ke Su[1,2], and Weili Zhou[1,2]

[1] Shanghai Astronomical Observatory,
Chinese Academy of Sciences, Shanghai 200030, China
slsong@shao.ac.cn
[2] University of Chinese Academy of Sciences, Beijing 100049, China

Abstract. This paper combines ten tropospheric combined empirical models based on the atmospheric element prediction model of GPT/GPT2, the Saastamoinen and the Modified Hopfield model and the mapping function of VMF1/GMF/NMF, and combines two tropospheric combined numerical weather prediction models based on the pressure-level data of ECMWF. This paper focuses on the impact of different tropospheric models on the positioning and zenith tropospheric delay (ZTD) accuracy of multi-GNSS precise point positioning (PPP) based on International GNSS Monitoring and Assessment System (iGMAS) products. The results show that the accuracy of GPT2 +Saastamoinen is 12.69% higher than UNB3M and the accuracy of Numerical Weather Model (NWM) is 63.80% higher than UNB3M based on the data of IGS ZTD. In terms of PPP positioning accuracy, the accuracy of GPT2+VMF1 +Modified Hopfield is 5.30% higher than UNB3M and the accuracy of NWM (GMF) is 8.77% higher than UNB3M. This paper gives a reference for the best empirical models of GPT2+VMF1+Modified Hopfield and the best numerical weather prediction model of NWM (GMF) and provides a more accurate tropospheric model for standard point positioning (SPP), PPP, and medium and long baseline positioning.

Keywords: iGMAS · GPT2 · ECMWF · NWM · Precise point positioning · Positioning accuracy · ZTD

1 Introduction

Tropospheric delay is one of the main error sources in GNSS positioning, which restricts the convergence time and positioning accuracy of GNSS precise point positioning (PPP) and medium or long baseline differential positioning [1]. Since the tropospheric delay is a non-dispersive delay and has nothing to do with the signal frequency, it cannot be eliminated by the linear combination of signals of different frequencies. Tropospheric delay can be divided into dry and wet components. The dry delay accounts for 90% of the total delay and the main physical properties of dry delay are related to the pressure, which can be accurately solved by the models. The wet delay accounts for only 10% of the total delay and it is difficult to model using surface meteorological data, because the distribution of water vapor in the atmosphere is

uneven and complex over time [2]. At this stage, the value of zenith troposphere delay (ZTD) calculated by empirical models is used as the initial value and the prior variance is set, and the bias is solved as an unknown parameter in PPP and long baseline differential positioning. However, the inaccurate prior variance will directly lead to divergence of the tropospheric and ambiguity parameters of the user station during the filtering process [3–5]. Hence, choosing an accurate tropospheric model as a priori information can improve the positioning accuracy of PPP and improve the convergence rate of PPP and the accuracy of ZTD. In the research of the tropospheric combined models, Xu et al. compared GPT2+GMF+Saastamoinen model with the meteorological data. It is concluded that the combined model can meet the requirements of high-precision positioning when meteorological data cannot be obtained [4]. Wang and Chen combined the GPT+NMF, GPT+GMF, GPT2+VMF1 models and test these combined models based on PPP. The result shows that the GPT+GMF and GPT2 +VMF1 is 22.0% higher than GPT+NMF [6]. Liu et al. combined GPT2/GPT2w +Saastamoinen model and compared it with IGS ZTD to conclude that the accuracy of GPT2w+Saastamoinen model is better than GPT2+Saastamoinen [7]. At this stage, the analysis of tropospheric combined models focused on the analysis of the precision of the troposphere model in the ZTD, and less consideration is given to the influence of different troposphere models on the accuracy of PPP positioning. Among the existing model combinations, most of them are based on the Saastamoinen model for calculation, and there are fewer combinations of other solution models. Among the existing model combinations, there are more combinations based on the GPT2 model, and less exploration of other metrological data, especially the Numerical Weather Model (NWM). In the research of real-time processing and post-processing of standard point positioning (SPP) and PPP, there are few papers that give a clear model of the optimal tropospheric combined model. Based on the model of GPT/GPT2/NWM combined the Saastamoinen model, the Modified Hopfield model and the mapping function of VMF1/GMF/NMF, this paper combines 12 tropospheric models. Based on iGMAS products, this paper explores the influence of tropospheric combined model on PPP positioning accuracy, and ZTD final estimation accuracy, in order to obtain the optimal combined model to provide a more accurate tropospheric model for users to perform SPP, PPP or medium and long baseline positioning.

2   Tropospheric Combined Models and Multi-GNSS PPP Model

2.1   Tropospheric Combined Models

2.1.1   Meteorological Data Models

In this paper, the meteorological data required for tropospheric solution is provided by GPT, GPT2 and NWMs. The GPT model is an empirical model based on the 3 years (September 1999 to August 2002) of $15° \times 15°$ global grids of monthly mean profiles for pressure and temperature from the European Centre for Medium-Range Weather Forecasts (ECMWF) 40 years reanalysis data (ERA40) [8].

$$P = P_r(1 - 0.0000226(h - h_r))^{5.225} \tag{1}$$

$$dT/dh = -0.0065° \, C/m \tag{2}$$

Then, the pressure values P on the Earth surface at height h are reduced to pressure values P_r at mean sea level (MSL) h_r and dT/dh is a linear decrease of temperature T with height [8]. The pressure and temperature at MSL are available from Eq. 3:

$$a = a_0 + A \cos\left(\frac{doy - 28}{365.25} \times 2\pi\right) \tag{3}$$

$$a_0 = \sum_{n=0}^{9} \sum_{m=0}^{n} P_{nm}(\sin \varphi)[A_{nm} \cos(m\lambda) + B_{nm} \sin(m\lambda)] \tag{4}$$

where P_{nm} denotes the Legendre polynomials, φ and λ are latitude and longitude, A_{nm} and B_{nm} are spherical harmonic coefficients.

The GPT2 model is an empirical model based on the 10 years (2001–2010) of global monthly mean profiles for pressure P, temperature T, specific humidity Q, and geopotential from ERA-Interim, discretized at 37 pressure levels and 1° of latitude and longitude. The GPT2 model can provide the meteorological parameters P, T, Q, the temperature lapse rate and the coefficients ah and aw of the hydrostatic and wet mapping functions of VMF1. At each grid point, each meteorological parameter $r(t)$ contains an annual term and a semi-annual term [9].

$$\begin{aligned} r(t) = A_0 + A_1 \cos\left(\frac{doy}{365.25} \times 2\pi\right) + B_1 \sin\left(\frac{doy}{365.25} \times 2\pi\right) \\ + A_2 \cos\left(\frac{doy}{365.25} \times 4\pi\right) + B_2 \sin\left(\frac{doy}{365.25} \times 4\pi\right) \end{aligned} \tag{5}$$

A_0, A_1, A_2, B_1, B_2 have been calculated in advance and stored in a text file in grid form. In the vertical direction, Lagler et al. assumed that the temperature near the earth follows a linear change with height, while the vertical change in pressure is expressed by an exponential function, and the following formula is used to correct the height of the meteorological parameters [9]:

$$\begin{cases} T = T_0 + dT/dh, P = P_0 \times e^{\frac{-c \times dh}{100}}, c = g_m \times \frac{dMtr}{R_g \times T_v}, \\ g_m = 9.784 \times (1.0 - 2.66 \times 10^{-3} \cos(2 \times lat) - 2.8 \times 10^{-7}h_s), \\ T_v = T_0 \times (1 + 0.6077Q), e = Q \times \frac{P}{0.622 + 0.378Q} \end{cases} \tag{6}$$

where T_0 and P_0 are temperature (K) and pressure (hPa) on grid, T and P are the temperature and pressure when the grid points increase the height of dh. dT is the temperature lapse rate, Q is specific humidity, e is water vapor pressure (hPa), g_m is gravitational acceleration, and its value is 9.80665 m/s², and $dMtr$ and R_g are

atmospheric molar masses and gas constants, respectively, with values of 0.028965 kg/mol and 8.3143 J/K/mol.

2.1.2   Tropospheric Models

The Saastamoinen model is a ZTD solution model based on the meteorological data of the station, which can be expressed as:

$$ZTD_{Saastamoinen} = 0.002277 \times \frac{P_{sta} + \left(0.05 + \frac{1255}{T_{sta}}\right)e}{f(\varphi, H)} \tag{7}$$

where P_{sta} is the surface pressure, T_{sta} is the surface temperature, e is the vaper pressure and $f(\varphi, H)$ is the mapping function. Saas is used to represent the Saastamoinen model unless otherwise specified below.

The Modified Hopfield model is a ZTD solution model based on the meteorological data of the station, which can be expressed as:

$$ZTD_{Modified\ Hopfield} = ZTD_{dry} + ZTD_{wet} \tag{8}$$

$$ZTD_i = 10^{-6} N_i \sum_{k=1}^{9} \frac{f_{k,i}}{k} r_i^k, i = dry, wet \tag{9}$$

$$
\begin{aligned}
&r_i = \sqrt{(R_E + h_i)^2 - R_E^2 \sin^2 z} - R_E \cos z \\
&f_{1,i} = 1, f_{2,i} = 4a_i, f_{3,i} = 6a_i^2 + 4b_i, f_{4,i} = 4a_i\left(a_i^2 + 3b_i\right) \\
&f_{5,i} = a_i^4 + 12a_i^2 b_i + 6b_i^2, f_{6,i} = 4a_i b_i\left(a_i^2 + 3b_i\right) \\
&f_{7,i} = b_i^2\left(6a_i^2 + 4b_i\right), f_{8,i} = 4a_i b_i^3, f_{9,i} = b_i^4 \\
&a_i = -\frac{\cos z}{h_i}, b_i = -\frac{\sin^2 z}{2h_i R_E} \\
&h_d = 40136 + 148.72(T_{sta} - 273.16), h_w = 11000 \\
&N_d = 77.64\frac{P_{sta}}{T_{sta}}, N_w = -12.96\frac{e}{T_{sta}} + 371800\frac{e}{T_{sta}^2}
\end{aligned}
\tag{10}
$$

where z is the zenith angle of satellite and R_E is the Earth radius. Hope is used to represent the Modified Hopfield model unless otherwise specified below.

The integration method is mainly used for the pressure-level data, which can be expressed as:

$$ZTD_{grid} = 10^{-6} \int_{H_{Station}}^{H_{top}} N dH = 10^{-6} \sum_i N_i \Delta H_i \tag{11}$$

where ZTD_{grid} is the ZTD value of the grid dot at the height of the IGS station, $H_{Station}$ is the elevation of the IGS station, H_{top} is the top-level height of the ECMWF meteorological data and N is the total refraction. The model of the total refraction can be expressed as:

$$N = k_1 \frac{P - e}{T} + k_2 \frac{e}{T} + k_3 \frac{e}{T^2} = N_{dry} + N_{wet} \qquad (12)$$

$$e = Sh \frac{P}{0.622 + 0.378Sh} \qquad (13)$$

where k_1 = 77.690 K/mbar, k_2 = 71.2952.79 K/mbar and k_3 = 375463.0 K^2/mbar [10], P is the atmospheric pressure, T is the temperature and Sh is the relative humidity. Integration is used to represent the integration model unless otherwise specified below. Based on the model of GPT/GPT2/NWM combined the Saastamoinen model, the Modified Hopfield model and the mapping function of VMF1/GMF/NMF, this paper combines 12 tropospheric models. The combined models will be shown in Fig. 1.
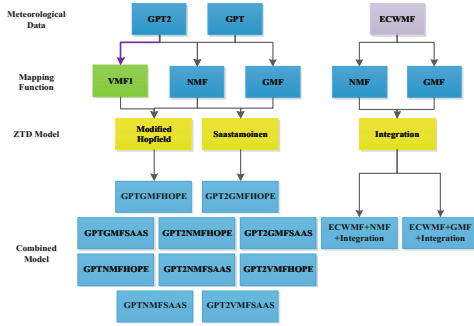

Fig. 1. Flow chart of calculation of tropospheric combined model

2.2 Multi-GNSS PPP Model

The PPP model used in this paper is ionosphere-free (IF) model. IF model uses dual-frequency pseudorange and carrier-phase observations of IF positioning model, which is expressed as follows [11]:

$$P_{IF} = \frac{f_1^2 \cdot P_1 - f_2^2 \cdot P_2}{f_1^2 - f_2^2} = \rho_r^s + c \cdot \delta t_r - c \cdot \delta t^s + T_r^s + \varepsilon_P \qquad (14)$$

$$\Phi_{IF} = \frac{f_1^2 \cdot \varphi_1 - f_2^2 \cdot \varphi_2}{f_1^2 - f_2^2} = \rho_r^s + c \cdot \delta t_r - c \cdot \delta t^s + T_r^s + \lambda_{r,IF} N_{r,IF}^s + \varepsilon_\Phi \qquad (15)$$

where P_{IF} is IF code observation, Φ_{IF} is the IF carrier-phase observation, ρ_r^s denotes the computed geometrical range, T_r^s is the tropospheric delay, N_r^s is the float ambiguity; ε_P and ε_Φ are the pseudorange and carrier phase observation noises including multipath, respectively. Based on the traditional single GNSS positioning model and taking into account the influence of inter-time bias and inter-frequency bias, the multi-GNSS PPP equation can be obtained by introducing an inter-system bias (ISB) for each additional system.

$$
\begin{cases}
P_r^G = \rho_r^s + c \cdot \delta t_r - c \cdot \delta t^s + T_r^s + \varepsilon_{P_r^G} \\
\Phi_r^G = \rho_r^s + c \cdot \delta t_r - c \cdot \delta t^s + T_r^s + \lambda_{r,IF} N_{r,IF}^s + \varepsilon_{\Phi_r^G} \\
P_r^C = \rho_r^s + c \cdot \delta t_r - c \cdot \delta t^s + c \cdot ISB_r^C + T_r^s + \varepsilon_{P_r^C} \\
\Phi_r^C = \rho_r^s + c \cdot \delta t_r - c \cdot \delta t^s + c \cdot ISB_r^C + T_r^s + \lambda_{r,IF} N_{r,IF}^s + \varepsilon_{\Phi_r^C} \\
P_r^{R_k} = \rho_r^s + c \cdot \delta t_r - c \cdot \delta t^s + c \cdot ISB_r^{R_k} + T_r^s + \varepsilon_{P_r^{R_k}} \\
\Phi_r^{R_k} = \rho_r^s + c \cdot \delta t_r - c \cdot \delta t^s + c \cdot ISB_r^{R_k} + T_r^s + \lambda_{r,IF} N_{r,IF}^s + \varepsilon_{\Phi_r^{R_k}} \\
P_r^E = \rho_r^s + c \cdot \delta t_r - c \cdot \delta t^s + c \cdot ISB_r^E + T_r^s + \varepsilon_{P_r^E} \\
\Phi_r^E = \rho_r^s + c \cdot \delta t_r - c \cdot \delta t^s + c \cdot ISB_r^E + T_r^s + \lambda_{r,IF} N_{r,IF}^s + \varepsilon_{\Phi_r^E}
\end{cases}
\tag{16}
$$

where the indices G, C, R and E refer to GPS, BDS, GLONASS and Galileo, respectively, ISB_r^C is the ISB between the BDS and GPS, ISB_r^E are the ISB between the Galileo and GPS, $ISB_r^{R_k}$ is the ISB between the GLONASS and GPS. Since the GLONASS uses signal deconstruction of frequency division multiple access (FDMA), the ISB of GLONASS is related to station R and satellite S.

3   Data Sets and Processing Strategy

The datasets utilized in this study are collected at 16 stations on 30 days, from January 1, 2018 to January 30, 2018. The experiment tests 30 days of observation data. All selected stations can receive the observations from GPS, BDS, GLONASS, and Galileo constellations. The observation data has a sampling interval of 30 s. Figure 2 shows the distribution of the selected station in multi-GNSS Experiment (MGEX). The orbit and clock offset of iGMAS integrated products have a sampling of 15 min and 5 min, respectively, and the time system of products is Beidou Time (BDT). In this paper, the pressure-level data of the ERA-Interim (Jan 1979-present) product from ECMWF are used. The horizontal resolution of the data is $0.125° \times 0.125°$, the vertical resolution is 37 pressure levels, and the time resolution is 6 h (0, 6, 12, 18 UTC).
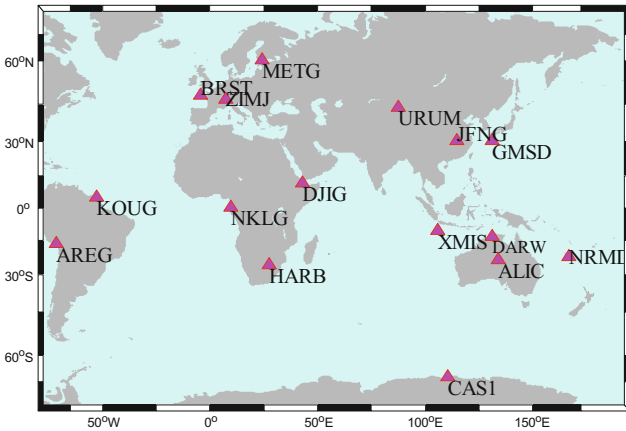

Fig. 2. Geographical distribution of the selective MGEX stations

The PPP model used in this paper is IF model. In IF model, the estimated parameters include the receiver position, the zenith wet tropospheric delay (ZWD), the receiver clock offset, the ISB, and the ambiguity. The 3-D position parameters (x, y, z) of the receiver are processed in static mode. The receiver clock error is treated as white noise. The Kalman filtering algorithm is applied in the multi-GNSS PPP processing. Phase Center Offset (PCO) and Phase Center Variations (PCV) of satellite and receiver antennas are corrected using the ANTEX file provided by IGS. Table 1 summarizes the detailed processing strategy for multi-GNSS PPP. In order to study the influence of different tropospheric models on the accuracy of PPP positioning, two methods of estimating ZWD and not estimating ZWD are used in this paper. Table 2 shows that the comparison of multi-GNSS PPP models with ZWD parameters. Table 3 shows that the comparison of multi-GNSS PPP models without ZWD parameters. Where m, n, p, q are the number of satellites for GPS, BDS, GLONASS, and Galileo, respectively. The model with ZWD parameters is one parameter less than the model without ZWD parameters and one more redundant observation.

Table 1. Multi-GNSS PPP processing strategy

Items	Model
Observations	Pseudorange and carrier-phase observations
Signal selection	G:L1/L2; C:B1/B2; R:G1/G2; E:E1/E5a
Sampling rate	30 s
Elevation cutoff	10°
Observation weighting	A priori precision 0.6 m and 0.004 m for code and phase observations, respectively [11]
Tropospheric delay	Tropospheric combined models
Ionospheric delay	Ionosphere-free linear combination
Satellite antenna	IGS ANTEX PCO+PCV
Receiver antenna	IGS ANTEX PCO+PCV
Phase windup effect	IERS2010 [14]
Earth rotation	IERS2010 [14]
Relativistic effect	IERS2010 [14]
Station displacement	Solid earth, pole and ocean tide (IERS2010) [14]
Receiver coordinate	Estimation
Receiver clock offset	Estimation
Troposphere	Estimation/no operation
ISB	Estimation
Ambiguity	Estimation

Table 2. The comparison of multi-GNSS PPP models with ZWD parameters

	G	G/C	G/R	G/E	G/C/R	G/R/E	G/C/R/E
Observed quantity	2m	2m + 2n	2m + 2p	2m + 2q	2m + 2n + 2p	2m + 2n + 2q	2m + 2n + 2p + 2q
Number of the parameter	m + 5	m + n + 6	m + p + 6	m + q + 6	m + n + p + 7	m + n + q + 7	m + n + p + q + 8
Redundancy	m − 5	m + n − 6	m + p − 6	m + q − 6	m + n + p − 7	m + p + q − 7	m + n + p + q − 8

Table 3. The comparison of multi-GNSS PPP models without ZWD parameters

	G	G/C	G/R	G/E	G/C/R	G/R/E	G/C/R/E
Observed quantity	2m	2m + 2n	2m + 2p	2m + 2q	2m + 2n + 2p	2m + 2n + 2q	2m + 2n + 2p + 2q
Number of the parameter	m + 4	m + n + 5	m + p + 5	m + q + 5	m + n + p + 6	m + n + q + 6	m + n + p + q + 7
Redundancy	m − 4	m + n − 5	m + p − 5	m + q − 5	m + n + p − 6	m + p + q − 6	m + n + p + q − 7

4   Data Tests and Results Analysis

4.1   The Analysis of the Accuracy of Tropospheric Models

This subsection studies the accuracy of the tropospheric combined models based on GPT, GPT2, and ECMWF meteorological data with Saastamoinen, Modified Hopfield, and integral models. The tropospheric combined models are compared with the UNB3M model commonly used in PPP to study the improvement rate of the tropospheric combination model compared to UNB3M model. Figure 3(a) shows the root mean square error (RMS) of the ZTD of the tropospheric combination model and the UNB3M model. It can be seen from Fig. 3 that the accuracy of the UNB3M model is lower than the tropospheric combination model and the NWM. The accuracy of the NWM is optimal and the accuracy of the NWM is 34.20 mm better than the UNB3M model. The accuracy of the tropospheric prior combination model is 3–7 mm better than the UNB3M model. Figure 3(b) shows the increasing rate of the accuracy of the tropospheric combined models compared to UNB3M model, and the specific rates are detailed in Table 4. From Fig. 3 and Table 4, it can be seen that the accuracy of the NWM model is higher than that of the UNB3M model, and its improvement rate is 63.81%. GPT+Modified Hopfield has a low rate of improvement, only 5.78%. From the perspective on the accuracy of the meteorological data, the pressure-level meteorological data provided by ECMWF is the best, the second is the GPT2 model, and the GPT and UNB3M models have less accurate meteorological data [12]. From the perspective on the accuracy of the ZTD calculated by the troposphere model, the accuracy of the Saastamoinen model is better than Modified Hopfield model.
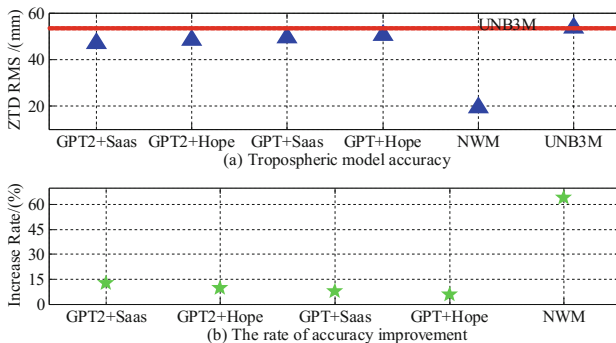
Fig. 3. The comparison of ZTD accuracy of tropospheric combined models

Table 4. The increase rate of ZTD accuracy of tropospheric combined models based on UNB3M

	GPT2+Saas	GPT2+Hope	GPT+Saas	GPT+Hope	NWM
Increase rate	12.69%	9.70%	7.65%	5.78%	63.81%

4.2 The Analysis of PPP Result Based on Tropospheric Models

In order to study the performance of the different tropospheric models in the positioning process, 12 tropospheric combined models for multi-GNSS PPP in this subsection were tested according to the processing strategies described in Sect. 3. Because the correlation relationship between the positioning accuracy in the Up direction and ZTD is strong and the correlation relationship between the positioning accuracy in the East and North direction and ZTD is weak [13], this section only gives the positioning accuracy in the Up direction to discuss the accuracy of the troposphere model.

Figure 4(a, b, c) shows the positioning accuracy in the Up direction based on the NMF, VMF1, and GMF mapping functions. Figure 4(d) shows the increasing rate of the positioning accuracy of the tropospheric combined models compared to UNB3M model in the Up direction. From the perspective on the accuracy of the mapping function, it can be seen that the mapping function of VMF1 has superior precision, the accuracy of the mapping function of GMF is weak, and the mapping function of NMF has poor accuracy. From the perspective on the accuracy of the calculation of multi-GNSS PPP, both the positioning accuracy in the Up direction and ZTD has improved. Because of the increase in the number of satellites, the optimization of the geometry of the satellites, the optimization of the observation conditions, and the increase in the number of redundant observations, the accuracy of PPP in the Up direction and the accuracy of ZTD have been have been improved. From the perspective on the accuracy of the meteorological data, Fig. 4(a, b) shows the positioning accuracy in the Up

direction using the NWM model is optimal and Fig. 5(a, c) shows the accuracy of ZTD estimated by Multi-GNSS PPP using the NWM model is optimal. From the PPP positioning accuracy and ZTD accuracy of the NMW model, it can be seen that the NWM meteorological data are more accurate, the second is the GPT2 model, the GPT and UNB3M models have less accurate meteorological data. From the perspective on the accuracy of the tropospheric model, Fig. 4(d) and Table 5 show the improvement rate of the positioning accuracy of the combination of NWM+GMF+integral is 8.77% compared to UNB3M model; The improvement rate of the positioning accuracy of the combination of GPT2+VMF1+Modified Hopfield is 5.30% compared to the UNB3M model in several prior tropospheric combined models. Under the condition of similar meteorological data model and similar mapping function, comparing the precision of the Modified Hopfield model and the Saastamoinen model, we can see that Table 5 shows the Modified Hopfield model is better than the Saastamoinen model in PPP solution process, and Table 4 shows the Saastamoinen model is better than the Modified Hopfield model in the process of solving the ZTD. To find out the reasons, ZWD is a more accurate value estimated by setting parameters, it is the zenith hydrostatic delay (ZHD) that really plays a role in the tropospheric model in PPP calculation. From this we can conclude that the Saastamoinen model is superior to the Modified Hopfield model in solving the ZTD, but the Modified Hopfield model is superior to the Saastamoinen model in solving the ZHD. The experiment shows that in the PPP post-processing process, the combination of NWM+GMF+Integral is optimal, and it's the positioning accuracy in the Up direction can be increased by 8.77%, and the accuracy of ZTD can be increased by 4.44%; In the real-time PPP processing process, the combination of GPT2+VMF1+Modified Hopfield is optimal, and the positioning accuracy in the Up direction can be increased by 5.30%, and the accuracy of ZTD can be increased by 0.25%.
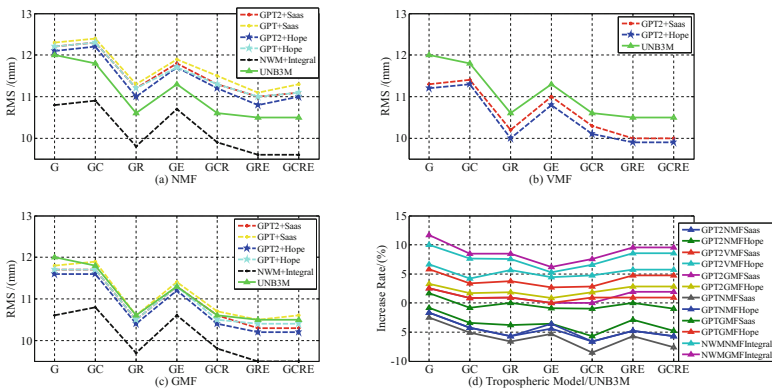

Fig. 4. The comparison of PPP up directional positioning accuracy of different tropospheric models with ZWD parameters

Table 5. The increasing rate of PPP up directional positioning accuracy of different tropospheric models based on UNB3M with ZWD parameters

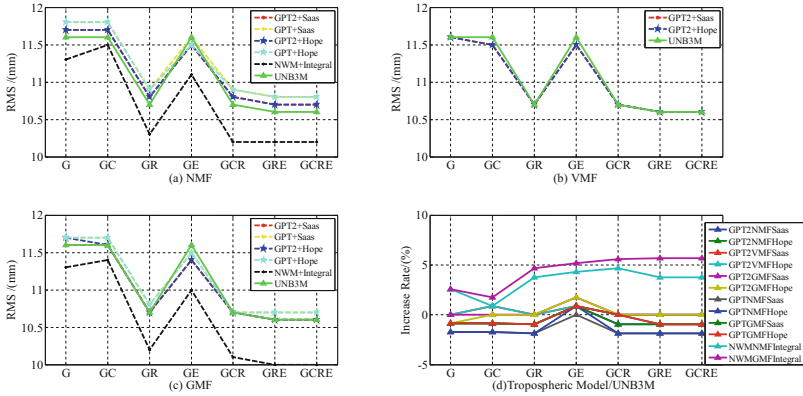| Mete	Mapping	Model	G	GC	GR	GE	GCR	GRE	GCRE	Mean
GPT2	NMF	Saas	−1.67%	−4.24%	−5.66%	−4.42%	−6.60%	−4.76%	−5.71%	−4.72%
		Hope	−0.83%	−3.39%	−3.77%	−3.54%	−5.66%	−2.86%	−4.76%	−3.55%
	VMF1	Saas	5.83%	3.39%	3.77%	2.65%	2.83%	4.76%	4.76%	4.00%
		Hope	6.67%	4.24%	5.66%	4.42%	4.72%	5.71%	5.71%	5.30%
	GMF	Saas	2.50%	0.85%	0.94%	0%	0%	1.90%	1.90%	1.16%
		Hope	3.33%	1.69%	1.89%	0.88%	1.89%	2.86%	2.86%	2.20%
GPT	NMF	Saas	−2.50%	−5.08%	−6.60%	−5.31%	−8.49%	−5.71%	−7.62%	−5.90%
		Hope	−1.67%	−4.24%	−5.66%	−3.54%	−6.60%	−4.76%	−5.71%	−4.60%
	GMF	Saas	1.67%	−0.85%	0%	−0.88%	−0.94%	0%	−0.95%	−0.28%
		Hope	2.50%	0.85%	0.94%	0%	0.94%	0.95%	0.95%	1.02%
NWM	NMF	Integral	10.00%	7.63%	7.55%	5.31%	6.60%	8.57%	8.57%	7.75%
	GMF	Integral	11.67%	8.47%	8.49%	6.19%	7.55%	9.52%	9.52%	8.77%

Fig. 5. The comparison of PPP ZTD accuracy with ZWD parameters

Table 6. The increasing rate of PPP ZTD accuracy of different tropospheric models based on UNB3M with ZWD parameters

Mete	Mapping	Model	G	GC	GR	GE	GCR	GRE	GCRE	Mean
GPT2	NMF	Saas	−0.86%	−0.86%	−0.93%	0.86%	−0.93%	−0.94%	−0.94%	−0.66%
		Hope	−0.86%	−0.86%	−0.93%	0.86%	−0.93%	−0.94%	−0.94%	−0.66%
	VMF1	Saas	0%	0.86%	0%	0.86%	0%	0%	0%	0.25%
		Hope	0%	0.86%	0%	0.86%	0%	0%	0%	0.25%
	GMF	Saas	0%	0%	0%	1.72%	0%	0%	0%	0.25%
		Hope	−0.86%	0%	0%	1.72%	0%	0%	0%	0.12%
GPT	NMF	Saas	−1.72%	−1.72%	−1.87%	0%	−1.87%	−1.89%	−1.89%	−1.57%
		Hope	−1.72%	−1.72%	−1.87%	0.86%	−1.87%	−1.89%	−1.89%	−1.44%
	GMF	Saas	−0.86%	−0.86%	−0.93%	0.86%	0%	−0.94%	−0.94%	−0.53%
		Hope	−0.86%	−0.86%	−0.93%	0.86%	0%	−0.94%	−0.94%	−0.53%
NWM	NMF	Integral	2.59%	0.86%	3.74%	4.31%	4.67%	3.77%	3.77%	3.39%
	GMF	Integral	2.59%	1.72%	4.67%	5.17%	5.61%	5.66%	5.66%	4.44%

In the case of setting parameters to estimate ZWD, ZWD is a more accurate value estimated by setting parameters. In the PPP process, it is the ZHD that really plays a role in the troposphere models. In order to more intuitively explain the accuracy of the tropospheric model (ZWD + ZHD) in the actual solution, this section uses PPP solutions without ZWD parameters. Figure 6 shows the positioning accuracy in the Up direction without ZWD parameters. From the perspective on the accuracy of the mapping function, since the ZWD parameter is not set, the mapping function does not work in the process of PPP calculation. From Fig. 6, it can be seen that the different mapping functions exhibit the same computational accuracy based on the same meteorological parameter model and the same computational model. From the perspective on the accuracy of the calculation in Multi-GNSS PPP, the solutions of different systems are relatively stable. From the perspective on the accuracy of the troposphere model, it can be seen that the NWM accuracy is optimal and the positioning accuracy in the Up direction is about 72.8% higher than that of the UNB3M model by comparing Fig. 6(a), (b) and (c). The GPT2+Saastamoinen model is the best in the prior tropospheric combination model, which is 22.66% higher than UNB3M. Combined with the analysis of the troposphere model accuracy in the Sect. 4.1, we can conclude that the NWM model has the highest accuracy; The GPT2+Saastamoinen model has the highest accuracy in the prior tropospheric combination model (Table 7).
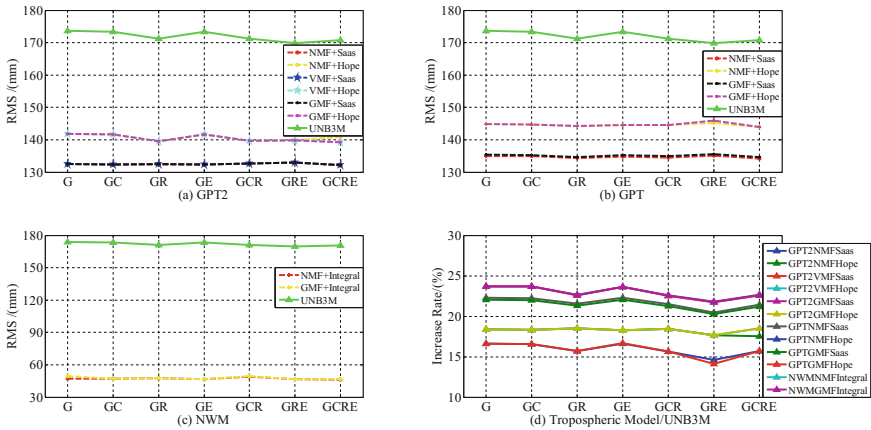

Fig. 6. The comparison of PPP up directional positioning accuracy of different tropospheric models without ZWD parameters

Table 7. The increasing rate of PPP up directional positioning accuracy of different tropospheric models based on UNB3M without ZWD parameters

Mete	Mapping	Model	G	GC	GR	GE	GCR	GRE	GCRE	Mean
GPT2	NMF	Saas	23.72%	23.70%	22.66%	23.64%	22.59%	21.78%	22.66%	22.97%
		Hope	18.36%	18.34%	18.52%	18.28%	18.45%	17.66%	17.51%	18.16%
	VMF1	Saas	23.72%	23.70%	22.61%	23.64%	22.53%	21.72%	22.60%	22.93%
		Hope	18.36%	18.34%	18.52%	18.28%	18.45%	17.66%	18.50%	18.30%
	GMF	Saas	23.72%	23.70%	22.61%	23.64%	22.53%	21.72%	22.60%	22.93%
		Hope	18.36%	18.34%	18.52%	18.28%	18.45%	17.66%	18.50%	18.30%
GPT	NMF	Saas	22.28%	22.20%	21.55%	22.26%	21.48%	20.48%	21.43%	21.67%
		Hope	16.64%	16.55%	15.71%	16.61%	15.65%	14.60%	15.69%	15.92%
	GMF	Saas	22.05%	21.97%	21.32%	22.03%	21.25%	20.25%	21.19%	21.44%
		Hope	16.64%	16.55%	15.71%	16.67%	15.65%	14.13%	15.69%	15.86%
NWM	NMF	Integral	72.94%	72.90%	72.25%	73.07%	71.28%	72.63%	72.89%	72.57%
	GMF	Integral	71.50%	72.78%	72.14%	72.95%	71.10%	72.51%	72.72%	72.24%

5   Conclusion

Based on the observation data of the MGEX station, this paper analyzes and compares the tropospheric model and mapping function in the aspects of both post process and real time. This paper compares the accuracy difference of different troposphere models from three aspects: the accuracy of the tropospheric combination models, the positioning accuracy on PPP Up direction and the accuracy of ZTD solution. We can come to the following conclusions.

1. From the perspective on the accuracy of the meteorological data, the accuracy of the pressure-level meteorological data provided by the ECMWF is the best, the second is the GPT2 model in the empirical model and the GPT and UNB3M models have less accurate meteorological data.
2. From the perspective on the accuracy of the calculation of multi-GNSS PPP, in the PPP post-processing process, the combination of NWM+GMF+Integral is optimal, and it's the positioning accuracy in the Up direction can be increased by 8.77%, and the accuracy of ZTD can be increased by 4.44%. In the real-time PPP processing process, the combination of GPT2+VMF1+Modified Hopfield is optimal, and it's the positioning accuracy in the Up direction can be increased by 5.30%, and the accuracy of ZTD can be increased by 0.25%.
3. From the perspective on the accuracy of the tropospheric model, the accuracy of the NWM model is the most obvious than that of the UNB3M model in the tropospheric combination model, and its improving rate is 63.81%; the accuracy of GPT2 +Saastamoinen is the most obvious than that of the UNB3M model in tropospheric empirical model, and its improvement rate is 63.81%; The Saastamoinen model is superior to the Modified Hopfield model in solving the ZTD, but the Modified Hopfield model is superior to the Saastamoinen model in solving the ZHD.

In summary, in the case of the PPP post-processing process, the tropospheric combination model of NWM+GMF+Integral can be used to improve the positioning and

ZTD accuracy. In the case of real-time PPP process, the GPT2+VMF1+Saastamoinen model can be used to improve the positioning and ZTD accuracy. The GPT2+VMF1 +Saastamoinen model can be used to improve the positioning accuracy without ZWD parameters such as SPP et al.

References

1. Song SL, Zhu WY, Chen QM et al (2011) Establishment of a new tropospheric delay correction model over China area. Sci China Phys Mech Astron 54:2271
2. Song SL, Zhu WY, Ding JC et al (2006) 3D water-vapor tomography with Shanghai GPS network to improve forecasted moisture field. Chin Sci Bull 51:607–614
3. de Oliveira PS, Morel L, Fund F et al (2017) Modeling tropospheric wet delays with dense and sparse network configurations for PPP-RTK. GPS Solut 21:237
4. Xu Y, Jiang N, Xu G, Yang Y, Schuh H (2015) Influence of meteorological data and horizontal gradient of tropospheric model on precise point positioning. Adv Space Res 56 (11):2374–2383
5. Yao YB, Zhang B, Yan F et al (2015) Two new sophisticated models for tropospheric delay corrections. Chin J Geophys 58(05):1492–1501 (in Chinese)
6. Wang J, Chen J, Wang J (2014) Analysis of tropospheric propagation delay mapping function models in GNSS. Prog Astron 32(03):383–394
7. Liu J, Chen X, Sun J, Liu Q (2016) An analysis of GPT2/GPT2w+Saastamoinen models for estimating zenith tropospheric delay over Asian area. Adv Space Res 59(3):824–832
8. Boehm J, Heinkelmann R, Schuh H (2007) Short note: a global model of pressure and temperature for geodetic applications. J Geodesy 81(10):679–683
9. Lagler K, Schindelegger M, Nilsson T et al (2013) GPT2: empirical slant delay model for radio space geodetic techniques. Geophys Res Lett 40(6):1069
10. Chen Q, Song S, Heise S et al (2011) Assessment of ZTD derived from ECMWF/NCEP data with GPS ZTD over China. GPS Solut 15:415
11. Cai C, Gao Y, Pan L, Zhu J (2015) Precise point positioning with quad-constellations: GPS, BeiDou, GLONASS and Galileo. Adv Space Res 56 https://doi.org/10.1016/j.asr.2015.04.001
12. Su K, Jin S (2018) Improvement of multi-GNSS precise point positioning performances with real meteorological data. J Navig 71(6):1363–1380
13. Li B, Feng Y, Shen Y, Wang C (2010) Geometry-specified troposphere decorrelation for subcentimeter real-time kinematic solutions over long baselines. J Geophys Res 115: B11404. https://doi.org/10.1029/2010JB007549
14. Petit G, Luzum B (2010) IERS conventions (No. IERS-TN-36). Bureau International Des Poids Et Mesures Sevres (France)